

Nanoscale

Accepted Manuscript



This is an *Accepted Manuscript*, which has been through the Royal Society of Chemistry peer review process and has been accepted for publication.

Accepted Manuscripts are published online shortly after acceptance, before technical editing, formatting and proof reading. Using this free service, authors can make their results available to the community, in citable form, before we publish the edited article. We will replace this *Accepted Manuscript* with the edited and formatted *Advance Article* as soon as it is available.

You can find more information about *Accepted Manuscripts* in the [Information for Authors](#).

Please note that technical editing may introduce minor changes to the text and/or graphics, which may alter content. The journal's standard [Terms & Conditions](#) and the [Ethical guidelines](#) still apply. In no event shall the Royal Society of Chemistry be held responsible for any errors or omissions in this *Accepted Manuscript* or any consequences arising from the use of any information it contains.

Simple top-down preparation of magnetic $\text{Bi}_{0.9}\text{Gd}_{0.1}\text{Fe}_{1-x}\text{Ti}_x\text{O}_3$ nanoparticles by ultrasonication of multiferroic bulk material

D.-T. Ngo

Department of Micro-and Nanotechnology, Technical University of Denmark, Kgs. Lyngby 2800, Denmark.

M. A. Basith* and A. Quader, M. A. Rahman

Department of Physics, Bangladesh University of Engineering and Technology, Dhaka-1000, Bangladesh.

B. L. Sinha

Department of Science and Humanities, MST, Dhaka, Bangladesh.

Bashir Ahmmad, Fumihiko Hirose

Graduate School of Science and Engineering, Yamagata University, 4-3-16 Jonan, Yonezawa 992-8510, Japan.

K. Mølhave

Department of Micro-and Nanotechnology, Technical University of Denmark, Lyngby 2800, Denmark.

(Dated: September 2, 2014)

We present a simple technique to synthesize ultrafine nanoparticles directly from bulk multiferroic perovskite powder. The starting materials, which were ceramic pellets of the nominal compositions of $\text{Bi}_{0.9}\text{Gd}_{0.1}\text{Fe}_{1-x}\text{Ti}_x\text{O}_3$ ($x = 0.00-0.20$), were prepared initially by a solid state reaction technique, then ground into micrometer-sized powders and mixed with isopropanol or water in an ultrasonic bath. The particle size was studied as function of time with transmission electron microscopic imaging, and electron diffraction confirmed the formation of a large fraction of single-crystalline nanoparticles with a mean size of 11-13 nm. A significant improvement in the magnetic behavior of $\text{Bi}_{0.9}\text{Gd}_{0.1}\text{Fe}_{1-x}\text{Ti}_x\text{O}_3$ nanoparticles compared to their bulk counterparts was observed at room temperature. This sonication technique may be considered as a simple and promising route to prepare ultrafine nanoparticles for functional applications.

PACS numbers:

I. INTRODUCTION

Multiferroic materials exhibit simultaneous presence of (anti)ferroelectricity, (anti)ferromagnetism, and/or ferroelasticity in the same phase [1–5]. The combination of 'ferro'-orders in multiferroics often means that the different properties interact with each other. This then allows the possibility that one can switch magnetically ordered states using electric fields or electrically ordered states using magnetic fields. These materials have attracted considerable research interest due to their potential applications in data storage, emerging field of spintronics, switchable spin valves, high frequency filters and sensors [6, 7]. Among the limited choices offered by the multiferroic materials, BiFeO_3 with rhombohedrally distorted perovskite structure is the most promising since it can exhibit multifunctional activities at room temperature (RT) [6, 7]. However, pure phase of BiFeO_3 is difficult to obtain [8, 9] and various impurity phases of bulk BiFeO_3 have been reported, mainly comprising of $\text{Bi}_2\text{Fe}_4\text{O}_9$, $\text{Bi}_{36}\text{Fe}_{24}\text{O}_{57}$ and $\text{Bi}_{25}\text{FeO}_{40}$ [10, 11]. Moreover, the bulk BiFeO_3 is characterized by serious current

leakage problems due to the existence of a large number of charge centres caused by oxygen ion vacancies [12–14]. Besides, in BiFeO_3 , magnetic ordering is of antiferromagnetic type, having a spiral modulated spin structure (SMSS) with an incommensurate long-wavelength period of 62 nm [12, 14]. This spiral spin structure cancels the macroscopic magnetization and prevents the observation of the linear magnetoelectric effect [15–17]. These problems ultimately limit the use of bulk BiFeO_3 in functional applications. It is evident that nanoparticles of BiFeO_3 , especially those with a particle size on the order of or smaller than the 62 nm SMSS exhibit improved ferroelectric and magnetic properties [4, 18–20].

Synthesis of BiFeO_3 multiferroic nanoparticles hence requires a particle size of the order or smaller than 62 nm [21]. To date, most of the published results reported the multiferroic properties of ceramics [8, 9] and thin film [22] systems of BiFeO_3 and it is still a challenge to synthesize BiFeO_3 nanostructures [7, 21, 23]. So far various chemistry based routes like the sol-gel method [18, 24], electro spray method [25], the combustion synthesis process [26], sonochemical synthesis process [27–29], were applied to synthesize multiferroic nanoparticles. Most of these chemical methods for the synthesis of multiferroic nanoparticles are either based on complex solution processes or involve toxic precursors [7].

This paper presents a simple route to prepare ultrafine

*Authors to whom correspondence should be addressed (e-mail): mabasith@phy.buet.ac.bd

nanoparticles from multiferroic $\text{Bi}_{0.9}\text{Gd}_{0.1}\text{Fe}_{1-x}\text{Ti}_x\text{O}_3$ ($x = 0.00, 0.10$ and 0.20) ceramics by the application of ultrasonic energy (a process called sonofragmentation). Sonofragmentation has been used to create nanoparticle dispersions from bulk powder producing nanoparticle fractions [30–32] and even inherently strong materials like carbon nanotubes can be fragmented by sonication [33]. In this investigation, nanoparticles were produced by using ultrasonic agitation without creating any chemical reactions. In a similar multiferroic system, the synthesis of undoped and Sc doped BiFeO_3 nanoparticles [28] (particle size 25–30 nm) was carried out using sonochemical technique which generates chemical reaction. The sonofragmentation technique is in fact a one-step synthesis technique to produce nanoparticles directly from bulk powders and might have the additional advantage that the chemistry of the particles likely will not be altered and hence bulk and nanoparticle materials will be more directly comparable in terms of multiferroic properties than materials produced by different synthesis methods. In our investigation, the magnetic properties of $\text{Bi}_{0.9}\text{Gd}_{0.1}\text{Fe}_{1-x}\text{Ti}_x\text{O}_3$ ($x = 0.00, 0.10$ and 0.20) nanoparticles synthesized by ultrasonication were investigated at room temperature and compared with their bulk counterparts. To estimate the concentration of oxygen vacancies in bulk polycrystalline samples as well as nanoparticles we have carried out X-ray photoelectron spectroscopy (XPS) analysis.

II. EXPERIMENTAL DETAILS

Ceramic pellets of multiferroics with nominal compositions of $\text{Bi}_{0.9}\text{Gd}_{0.1}\text{Fe}_{1-x}\text{Ti}_x\text{O}_3$ ($x = 0.0, 0.1$ and 0.2) were prepared by conventional solid state reaction technique. Details of the preparation process were described in our previous work published elsewhere [34]. Scanning Electron Microscopy (SEM) imaging confirmed surface morphology of the pellets with micron-sized grains [34]. The pellets were then ground into powder by performing manual grinding for 15 minutes. The obtained powders were subsequently mixed with isopropanol with a ratio of 50 mg powder and 10 ml isopropanol with a mass percentage of $\sim 0.5\%$. Then, the mixtures of isopropanol and powder were put into an ultrasonic bath. The sonication time was varied from 15 to 60 minutes. After 6 hours, $\sim 78\%$ of the mass had precipitated and the supernatant was used for transmission electron microscopy (TEM) investigation. Morphology and physical structure of the nanoparticles were studied using a FEI TECNAI TEM with a 200 kV accelerated voltage. For magnetic measurements, the particles in the solution were dried naturally to a condensed pellet. The magnetic properties of the nanoparticles were measured using an alternating gradient force magnetometer (AGFM) with a maximum applied field of 20 kOe. The magnetic moment was calibrated using a Ni standard specimen. To estimate the concentration of oxygen vacancies X-ray photoelectron

spectroscopy (XPS, ULVAC-PHI Inc., Model 1600) analysis was carried out with a Mg- $K\alpha$ radiation source.

III. RESULTS AND DISCUSSIONS

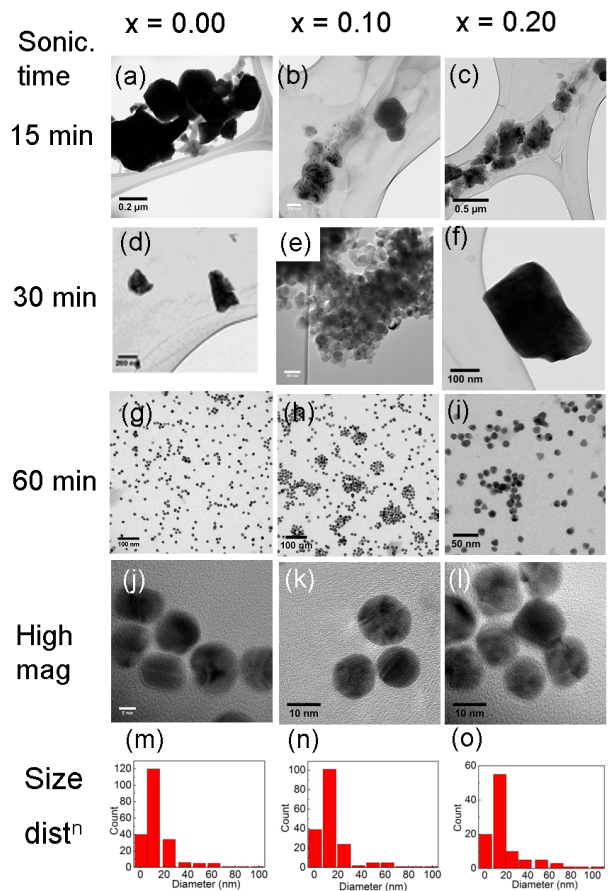


FIG. 1: BF TEM images of the $\text{Bi}_{0.9}\text{Gd}_{0.1}\text{Fe}_{1-x}\text{Ti}_x\text{O}_3$ ($x = 0.00-0.20$) particles obtained at various sonication time: (a-c) 15 minutes, (d-f) 30 minutes, (g-i) 60 minutes. (j, k and l) are the HRTEM images obtained at 60 mins of sonication. The plots (m, n and o) show distribution of nanoparticles deduced from frames (g, h and i), respectively.

Figure 1 shows bright-field (BF) TEM images of $\text{Bi}_{0.9}\text{Gd}_{0.1}\text{Fe}_{1-x}\text{Ti}_x\text{O}_3$ ($x = 0.00-0.20$) particles obtained at various sonication time: (a-c) 15 minutes, (d-f) 30 minutes and (g-i) 60 minutes. The left, middle and right columns are for compositions $x = 0.00, x = 0.10$ and 0.20 , respectively. Figures 1 (a-c) present the state in which the manually-ground powder was mixed with isopropanol in ultrasound, and the large-grain size powders started to break into smaller grain with the aid of the mechanical energy from the ultrasonic wave. In a short time of sonication (15 minutes), the grains were just about to be broken into sub-micron particles, however, still condensed together like micrometer sized particles [Figs. 1(a-c)]. As soon as the time of sonication was increased to 30 min-

utes, the particles started to separate from each other and thereby their sizes were decreased [Figs. 1(d-f)]. The sonication time was increased then to 60 minutes and this resulted in ultrafine and isolated nanoparticles with a very narrow distribution of average sizes around 11 ± 2 nm for $x = 0.00$, 12 ± 2 nm for $x = 0.10$, and 13 ± 2 nm for $x = 0.20$ compositions as shown in TEM images Figs. 1 (g-i), respectively. Figures 1 (j, k and l) demonstrate high resolution (HR) TEM images of the $\text{Bi}_{0.9}\text{Gd}_{0.1}\text{Fe}_{1-x}\text{Ti}_x\text{O}_3$ ($x = 0.00-0.20$) nanoparticles obtained at 60 minutes of sonication. These HRTEM images [Figs. 1 (j, k and l)] are a clear evidence of the ultrafine single crystal nanoparticles synthesized using a sonication time of 60 minutes. Figures 1(m, n and o) show the distribution of the synthesized nanoparticles deduced from images (g, h and i), respectively.

Figure 2(a) shows selected area electron diffraction (SAED) patterns of the $\text{Bi}_{0.9}\text{Gd}_{0.1}\text{Fe}_{1-x}\text{Ti}_x\text{O}_3$ with $x = 0.00$ particles (notably, $x = 0.00$ is the Ti undoped $\text{Bi}_{0.9}\text{Gd}_{0.1}\text{FeO}_3$ composition throughout the investigation) obtained after a sonication time of 30 minutes. This is the state which confirms a rhombohedral [20] structure of the isolated particles. The discontinuous diffraction rings also indicates single crystalline particles breaking up into smaller single crystalline nanoparticles. Figure 2(b) illustrates SAED of the $\text{Bi}_{0.9}\text{Gd}_{0.1}\text{Fe}_{1-x}\text{Ti}_x\text{O}_3$ ($x = 0.00$) nanoparticle (first column in Fig. 1) sonicated at 60 minutes and demonstrates clearly multiple peaks of monocrystalline patterns. The diffraction rings of SAED pattern in this state are well-defined and in good agreement with the rhombohedral structure of the nanoparticles with lattice constant of $a = 0.56$ nm, and $\alpha = 59.4$ degree obtained by indexing the SAED pattern. These values are quite consistent with the recent results of the BiFeO_3 nanoparticles [35, 36] synthesized by wet chemical techniques. This indicates that the rhombohedral crystal structure of the bulk BiFeO_3 [6, 7] remained unaltered in these synthesized nanoparticles. The HRTEM images demonstrate of a monocrystalline particle (Fig. 2(c)) and the existence of twin stacking faults (Fig. 2(d)) in the synthesized nanoparticles. These crystallographic stacking faults could also enhance the magnetic properties of the nanoparticles [37–39]. The stacking faults were also reported to relax the strain in the nanoparticles [37, 38], thus influence the magnetoelastic energy. In some cases, this would help to enhance the anisotropy of the nanoparticles [38, 39], especially in nanoparticles with ferromagnetic spin structure that we show below these particles have.

The effect of sonication time to breakdown micrometer sized particles was also demonstrated. Figure 2(e) shows the variation of the size of $\text{Bi}_{0.9}\text{Gd}_{0.1}\text{Fe}_{1-x}\text{Ti}_x\text{O}_3$ ($x = 0.0$) nanoparticle as a function of sonication time for a fixed power of the ultrasonic bath (50 W). We have observed clearly that a sonication time of 60 minutes was sufficient to produce monocrystalline nanoparticles. A further increment of the sonication time up to 90 minutes does not causes notable changes in the average size

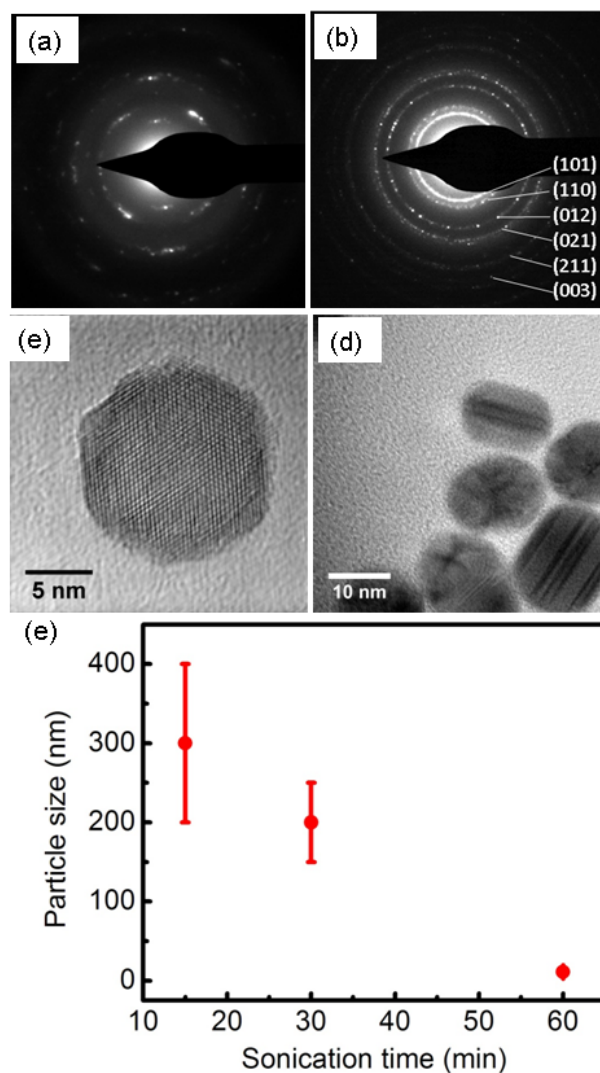


FIG. 2: (a) The SAED patterns of the $\text{Bi}_{0.9}\text{Gd}_{0.1}\text{Fe}_{1-x}\text{Ti}_x\text{O}_3$ ($x = 0.0$) particles sonicated 30 minutes showing discontinuous rings. Detailed TEM investigation of the $\text{Bi}_{0.9}\text{Gd}_{0.1}\text{Fe}_{1-x}\text{Ti}_x\text{O}_3$ ($x = 0.00$) nanoparticle (first column in Fig. 1) sonicated at 60 minutes are given in images (b-d). (b) SAED of nanoparticles showing multiple peaks of monocrystalline patterns. (c) HRTEM showing monocrystalline particle. (d) HRTEM showing twin stacking in single particle. (e) The variation of particle size as a function of sonication time for a fixed sonication power.

of the synthesized nanoparticles. The asymptotic behavior in Fig. 2(e) indicates that within the studied time frame, sonication induced aggregation of the nanoparticles is not occurring [40].

The yield of nanoparticles was estimated by measuring the mass of precipitate and supernatant after leaving the sonicated dispersion to settle for 6 hours where 22 % of the initial powder mass was converted into the supernatant fraction containing nanoparticles. Prior to these measurements the precipitate and supernatant were dried at 105°C for 2.5 hours.

The structural analysis of the $\text{Bi}_{0.9}\text{Gd}_{0.1}\text{Fe}_{1-x}\text{Ti}_x\text{O}_3$ ($x = 0.10$ and 0.20) nanoparticles sonicated at 60 minutes were also performed by capturing SAED patterns (images not shown here). Indexing the SAED patterns of the nanoparticles also ensured the rhombohedral structure of the $\text{Bi}_{0.9}\text{Gd}_{0.1}\text{Fe}_{0.9}\text{Ti}_{0.1}\text{O}_3$ and $\text{Bi}_{0.9}\text{Gd}_{0.1}\text{Fe}_{0.8}\text{Ti}_{0.2}\text{O}_3$ nanoparticles with the lattice constants of $a = 0.55$ nm, and 0.54 nm; and $\alpha = 59.3$, and 59.3 deg, respectively. The rhombohedral structure with reduced lattice constants due to the substitution of Ti for Fe is consistent with recent results [34–36] on the doped BiFeO_3 multiferroics.

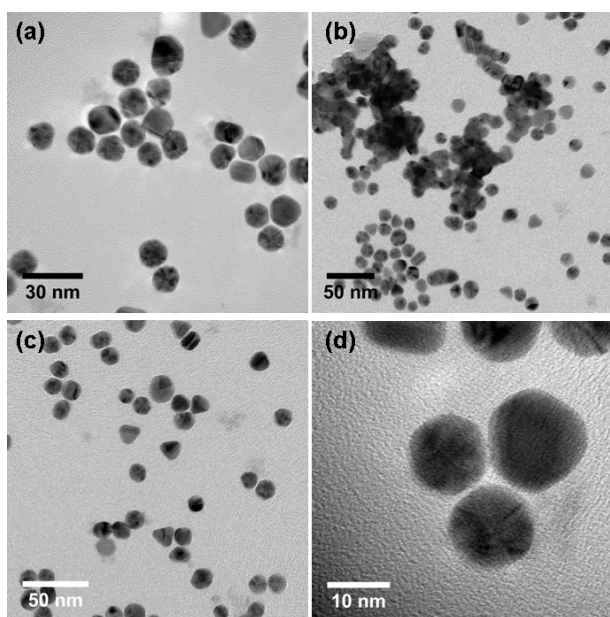


FIG. 3: TEM images of the $\text{Bi}_{0.9}\text{Gd}_{0.1}\text{Fe}_{1-x}\text{Ti}_x\text{O}_3$ nanoparticles obtained at 60 minutes of sonication in distilled water: (a) $x = 0.00$, (b) $x = 0.10$, (c) $x = 0.20$. The frame (d) is a HRTEM image of the nanoparticles in frame (c).

It is interesting to notice that similar evolution also occurs when we use distilled water instead of isopropanol to mix the powder in ultrasonic cleaner. The TEM images of the $\text{Bi}_{0.9}\text{Gd}_{0.1}\text{Fe}_{1-x}\text{Ti}_x\text{O}_3$ ($x = 0.00 - 0.20$) nanoparticles sonicated for 60 minutes using distilled water are shown in Figs. 3 (a-c): (a) $x = 0.00$, (b) $x = 0.10$, (c) $x = 0.20$. The frame (d) is a HRTEM image of the nanoparticles in frame (c). The average size of the synthesized nanoparticles is 13 ± 2 nm if we mix the powders with distilled water instead of isopropanol. Notably, use of distilled water instead of isopropanol for the production of stable nanoparticles does not cause any difference in sonication time and the optimum sonication time is again 60 minutes.

In the next stage of this investigation, magnetization versus magnetic field (M-H) hysteresis loops were carried out and results were displayed in Fig. 4. The inset of Fig. 4 also demonstrates M-H hysteresis loops of the bulk polycrystalline ceramics $\text{Bi}_{0.9}\text{Gd}_{0.1}\text{Fe}_{1-x}\text{Ti}_x\text{O}_3$ ($x =$

$0.00-0.20$) [34]. The obtained nanoparticles are expected to exhibit excellent properties, either ferromagnetics or ferroelectrics. Indeed, the nearly saturated M-H hysteresis loops of the synthesized nanoparticles clearly demonstrate improved magnetic properties compared to that of bulk ceramics [Fig. 4]. Notably, the bulk polycrystalline $\text{Bi}_{0.9}\text{Gd}_{0.1}\text{Fe}_{1-x}\text{Ti}_x\text{O}_3$ ceramics exhibit an almost linear relationship between the magnetic field and the magnetization [34] as was shown in the inset of Fig. 4. This is the expected behaviour for an antiferromagnet below T_{Neel} . Compared to the bulk ceramic samples [34], these nanoparticles possess much higher saturation magnetization M_s . The M_s value was determined from the intercept of two linear lines drawn through the low- and high-field regions of the M-H hysteresis loops [41]. The calculated values of M_s along with remanent magnetization (M_r) and coercivity (H_c) of $\text{Bi}_{0.9}\text{Gd}_{0.1}\text{Fe}_{1-x}\text{Ti}_x\text{O}_3$ ($x = 0-0.20$) nanoparticles are inserted in table 1. This table also displays the corresponding M_s , M_r and H_c values of the bulk $\text{Bi}_{0.9}\text{Gd}_{0.1}\text{Fe}_{1-x}\text{Ti}_x\text{O}_3$ ceramics observed in Ref. [34]. Furthermore, the M-H hysteresis loops of the synthesized nanoparticles exhibit a single-phase-like magnetization behaviour compared to the linear curve of the bulk, and this ultimately indicate qualitatively that a large fraction of the ultrasonicated specimen was converted into nanoparticles from bulk powders.

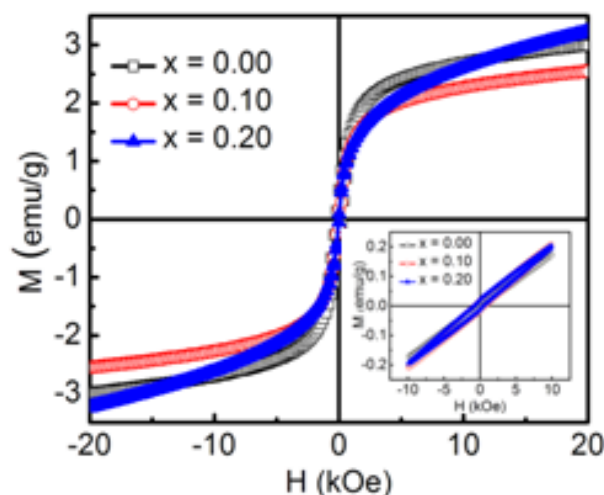


FIG. 4: Hysteresis loops of the $\text{Bi}_{0.9}\text{Gd}_{0.1}\text{Fe}_{1-x}\text{Ti}_x\text{O}_3$ ($x = 0-0.20$) nanoparticles obtained after a sonication time of 60 minutes. The inset shows hysteresis loops of the bulk samples.

Our results can be compared to a recent study where single crystalline BiFeO_3 nanoparticles were synthesized using facile sol-gel methodology based on the glycol gel reaction [18]. The highest M_s for BiFeO_3 nanoparticles was 1.55 emu/g at 50 kOe with an average particle size of 14 nm [18]. The M_s of Gd doped multiferroic $\text{Bi}_{0.9}\text{Gd}_{0.1}\text{FeO}_3$ nanoparticles synthesized by polyol-mediated method [20] with an average particle size of 34 nm was 0.75 emu/g at 30 kOe [20]. Notably, in this present investigation, the M_s for $\text{Bi}_{0.9}\text{Gd}_{0.1}\text{FeO}_3$

nanoparticles is 2.50 emu/g at 20 kOe for an average particle size of 11 ± 2 nm and this is much higher compared to the values observed in Refs. [18] and [20]. The large value of magnetization may be associated with their reduced particle size as was observed in Ref. [18] for single crystalline multiferroic BiFeO₃ nanoparticles. As was mentioned earlier, the magnetic ordering of BiFeO₃-based multiferroic ceramics is antiferromagnetic with a spiral modulated spin structure [12, 14, 42] and an incommensurate long-wavelength period of 62 nm. The enhanced magnetic properties in these nanoparticles could be explained as : i) due to the modification of the long range spiral-modulated spin structure of BiFeO₃ the ferromagnetic properties were enhanced for the synthesized nanoparticles with sizes much smaller than 62 nm [18] ii) the ionic radius of Gd³⁺ (0.938 Å) ion is much smaller than that of Bi³⁺ (1.17 Å) ion which may also lead to large distortion in lattice structure thereby leading to reduction of spiral spin modulation in BiFeO₃ [20] ; and iii) Gd³⁺ is magnetically active (effective magnetic moment is 8.0 Bohr Magnetron) and the ferromagnetic coupling between Gd³⁺ and Fe³⁺ ions may contribute significantly to enhance the magnetization [20].

In the case of bulk ceramics as well as nanoparticles, several authors reported that due to co-doping both in the Bi and Fe sites of BiFeO₃, multiferroic properties can be improved significantly [12, 44]. In a related system, Pb and Ti co-doped nanocrystalline Bi_{0.9}Pb_{0.1}Fe_{0.9}Ti_{0.1}O₃ multiferroics were prepared by solution combustion synthesis method from an α -alanine containing precursor [44] for which the M_s value was 0.60 emu/g at 40 kOe. In the investigation reported here, for 10 % Gd and Ti co-doped Bi_{0.9}Gd_{0.1}Fe_{0.9}Ti_{0.1}O₃ nanoparticles a well defined ferromagnetic hysteresis loop was observed in which the room temperature M_s is 2.3 emu/g at 20 kOe. Both M_s and M_r of Bi_{0.9}Gd_{0.1}Fe_{0.9}Ti_{0.1}O₃ nanoparticles are much higher compared to that of sonochemically synthesized Bi_{0.9}Fe_{0.95-x}Sc_{0.05}Ti_xO₃ nanoparticles reported in a recent investigation [45].

In the case of bulk polycrystalline ceramics, due to the presence of magnetic secondary phases, M_s , M_r and H_c were increased with the substitution of nonmagnetic Ti in place of Fe [34]. On the contrary, in phase pure single crystalline nanoparticles, the substitution of nonmagnetic Ti reasonably decreased M_s , M_r and H_c although the net value of the saturation magnetization was always higher for each composition compared to that of bulk ceramics. The coercivity was found to be reduced for these nanoparticles compared to that of bulk ceramic samples as was also observed for the reduced size single crystalline BiFeO₃ nanoparticles [18]. This indicates that the magnetic properties of these nanoparticles are related with their reduced size and crystallinity as was also determined in similar nanostructures [18, 20, 44]. Compared to the bulk ceramics, the coercive fields of the synthesized nanoparticles are much smaller and almost negligible for Bi_{0.9}Gd_{0.1}Fe_{1-x}Ti_xO₃ ($x=0.20$) nanoparticles (Table 1). This actually indicates their soft nature

and better suitability for device applications [46].

TABLE I: The table shows the comparison of the M_s , M_r and H_c between Bi_{0.9}Gd_{0.1}Fe_{1-x}Ti_xO₃ nanoparticles and bulk ceramics [34] observed at room temperature.

Ti concentration	M_s (emu/g)		M_r (emu/g)		H_c (Oe)	
	Nano	Bulk	Nano	Bulk	Nano	Bulk
0.00	2.50	–	0.46	0.006	238	345
0.10	2.10	–	0.11	0.02	53	836
0.20	2.05	–	0.003	0.02	6.5	820

Notably, the perovskite manganites nanoparticles of various compositions were also synthesized directly from bulk powder using top-down approach based on ball milling [48, 49]. The longer milling time produced successfully nanoparticles from a few nanometers to hundred nanometers, however, the magnetic properties of the fine particles were found to degrade [48]. This might be associated with the contamination and amorphization of fine particles during the milling process [50]. Although our material system is different, however, the findings of our investigation indicate the potentiality of the ultrasonication technique compared to mechanical milling for the preparation of phase pure nanoparticles which exhibit enhanced magnetic properties with size reduction.

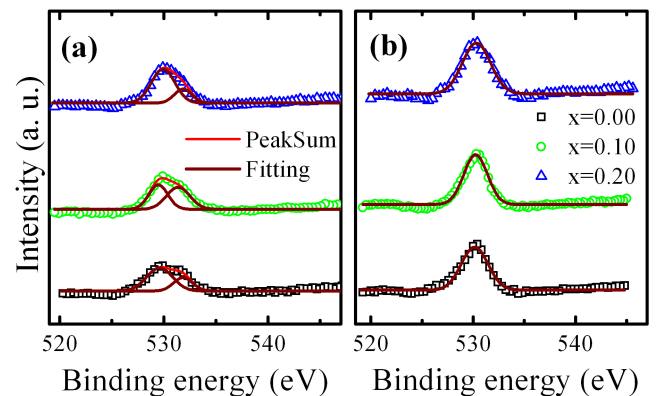


FIG. 5: XPS spectra of the O 1s of Bi_{0.9}Gd_{0.1}Fe_{1-x}Ti_xO₃ ($x=0-0.20$) (a) bulk polycrystalline materials and (b) nanoparticles obtained after a sonication time of 60 minutes.

As was mentioned earlier, the bulk BiFeO₃ is characterized by serious current leakage problems due to the existence of a large number of charge centres caused by oxygen ion vacancies [12, 51] that degrades the ferroelectric properties. Therefore, to further confirm the concentration of oxygen vacancies in the bulk polycrystalline ceramics and nanoparticles of Bi_{0.9}Gd_{0.1}Fe_{1-x}Ti_xO₃ ($x=0.00, 0.10, 0.20$) XPS measurements were also carried out. As presented in Fig. 5 (a), the O 1s XPS spectra of bulk polycrystalline Bi_{0.9}Gd_{0.1}Fe_{1-x}Ti_xO₃ ($x=0.00, 0.10, 0.20$) ceramics show a slightly asymmetric peak very close to 530 eV along with additional peak.

The asymmetric curves of the bulk samples can be Gaussian fitted by two symmetrical peaks at 529.8 eV and 532 eV, respectively. The lower binding energy peak at 529.8 eV is correspond the O 1s core spectrum, while higher binding energy peak is related to the oxygen vacancy [27, 52] in the sample. Interestingly, in the case of $\text{Bi}_{0.9}\text{Gd}_{0.1}\text{Fe}_{1-x}\text{Ti}_x\text{O}_3$ ($x = 0.00, 0.10, 0.20$) nanoparticles we have observed a symmetrically single XPS peak (Fig. 5 (b)) of O 1S at 530 eV [28, 45]. This indicates the absence of oxygen vacancy in $\text{Bi}_{0.9}\text{Gd}_{0.1}\text{Fe}_{1-x}\text{Ti}_x\text{O}_3$ ($x = 0.00, 0.10, 0.20$) nanoparticles. The absence of oxygen vacancies might reduce the leakage currents [45] and therefore, we may expect improved ferroelectric properties of the synthesized nanoparticles in subsequent investigations.

IV. CONCLUSIONS

We have employed successfully a cost effective simple top-down approach to prepare ultrafine $\text{Bi}_{0.9}\text{Gd}_{0.1}\text{Fe}_{1-x}\text{Ti}_x\text{O}_3$ ($x = 0.00-0.20$) nanoparticles directly from bulk powder without using any chemical solution processes as well as toxic precursors. HRTEM imaging as well as electron diffraction techniques confirmed single crystal rhombohedral structure of these synthesized nanoparticles. Comparatively a long time of sonication of around 60 minutes allows fabricating ultrafine nanoparticles with narrow size distribution ranging from 11 nm to 13 nm. Magnetic measurements demonstrate the enhanced magnetic properties of the nanoparticles compared to that of bulk materials, which may be referred to as room temperature ferromagnetism caused by the size reduction.

It is worth mentioning that to understand completely the behaviour of any material system at nanoscale it is worthwhile to know the behaviour of their bulk counterparts. Traditionally, to synthesize a multiferroic material system like $\text{Bi}_{1-x}\text{Gd}_x\text{FeO}_3$ bulk polycrystalline samples are prepared by a solid state reaction technique using bismuth oxide, ferric oxide and gadolinium oxide as a starting raw materials [53] whereas to synthesize the nanopar-

ticles of the same material system using a wet chemical technique like the sol-gel method where bismuth nitrate, ferrite nitrate and gadolinium nitrate are use as a starting raw materials [20]. The sonication technique provides the opportunity to synthesize both bulk polycrystalline samples as well as nanoparticles of the material system using the same route and same starting raw materials. Therefore, the comparison of the behaviour of the polycrystalline samples and nanoparticles become simple and reasonable. The product nanoparticles appear to have a good monodispersity with improved physical properties: the size, crystallinity and improved magnetic behavior of the synthesized nanoparticles at room temperature compared to the bulk starting material. This method might be analogous to surfactant assisted ball milling creating magnetic nanoparticles [47], a technique which demonstrated a narrow size distribution of the synthesized particles with increasing milling time [48, 49]. The very narrow and small size distribution achieved in the present study are surprising when comparing to the broader and larger size distributions achieved in other sonofragmentations studies of other materials [30–32, 54], but these results may first of all be material specific, and then the detection methods (SEM and various light scattering methods) employed in these previous studies are not always optimal to measure nanoparticles in the ~ 10 nm size range found here. More detailed studies of the particle fragmentation would be relevant to include in future studies along with evaluation of the particles possible multiferroic properties by Polarization vs Electric field (P-E) hysteresis loop measurements [20, 24, 28, 36, 45]. We conclude that this simple top-down preparation technique of ultrafine nanoparticles may be developed as a versatile technique for the preparation of other materials in general.

V. ACKNOWLEDGEMENTS

University Grants Commission, Dhaka and Bangladesh University of Engineering and Technology (BUET) for financial assistance.

-
- [1] W. Eerenstein, N. D. Mathur, J. F. Scott, *Nature*, 2006, **442**, 759.
 - [2] S. W. Cheong, M. Mostovoy, *Nature Materials*, 2007 **6**, 13-19.
 - [3] R. Ramesh, *Nature*, 461, **1218**, (2009).
 - [4] K. F. Wang, J. M. Liu, Z. F. Ren, *Adv. Phys.*, 2009, **58**, 321-448.
 - [5] J. T. Heron, D. G. Schlom, and R. Ramesh, *App. Phys. Rev.* 2014, **1**, 021303-18.
 - [6] V. V. Lazenka, G. Zhang, J. Vanacken, I. I. Makoed, A. F. Ravinski, V. V. Moshchalkov, *J. Phys. D: Appl. Phys.*, 2012, **45**, 125002-7.
 - [7] M. S. Bernardo, T. Jardim, M. F. Peiteado, J. Mompean, M. Garcia-Hernandez, M. A. Garcia, M. Villegas, A. C. Caballero, *Chem. Mater.*, 2013, **25**, 1533-1541.
 - [8] Q. H. Jiang, C. W. Nan, *J. Am. Ceram. Soc.*, 2006, **89**, 2123-2127.
 - [9] S. Ghosh, A. S. Dasgupta, H. S. Maiti, *J. Am. Ceram. Soc.*, 2005, **88**, 1349-1352.
 - [10] T. Munoz, J. P. Rivera, A. Monnier, H. Schmid, *Jpn. J. Appl. Phys. Part 1*, 1985, **24**, 1051-1053.
 - [11] M. Kumar, K. L. Yadav, *J. Appl. Phys.*, 2006, **100**, 074111-4.
 - [12] R. A. Agarwal, S. S. Ashima, N. Ahlawat, *J. Phys. D: Appl. Phys.*, 2012, **45**, 165001-9.
 - [13] X. Qi, J. Dho, R. Tomov, M. G. Blamire, J. L.

- MacManus-Driscoll, *App. Phys. Lett.* 2005, **86**, 062903-3.
- [14] P. Fischer, M. Polomska, I. Sosnowska, M. Szymanski, *J. Phys. C*, 1980, **13**, 1931-1940.
- [15] G. Catalan, J. F. Scott, *Adv. Mater.*, 2009, **21**, 2463-2485.
- [16] I. Sosnowska, T. P. Neumaier, Steichele, *J. Phys. C: Solid State Phys.* 1982, **15**, 4835-4846.
- [17] C. Ederer, N. A. Spaldin, *Phys. Rev. B*, 2005, **71**, 060401(R)-4.
- [18] T. J. Park, Georgia C. A. Papaefthymiou, A. J. Viescas, A. R. Moodenbaugh, S. S. Wong, *Nano Lett.*, 2007, **7** (3), 766-772.
- [19] A. Jaiswal, R. Das, K. Vivekanand, P. M. Abraham, S. Adyanthaya, P. Poddar, *J. Phys. Chem. C*, 2010, **114**, 2108-2115.
- [20] W. Hu, Y. Chen, H. Yuan, G. Li, Y. Qiao, Y. Qin, S. Feng, *J. Phys. Chem. C*, 2011, **115**, 8869-8875.
- [21] F. Huang, Z. Wang, X. Lu, J. Zhang, K. Min, W. Lin, R. Ti, T. Xu,; J. He, C. Yue, J. Zhu, *Scientific Reports*, 2013, **3**, 2907.
- [22] S. Gupta, M. Tomar, V. Gupta, *J. App. Phys.*, 2014, **115**, 014102-9.
- [23] N. Nuraje, and K. Su, *Nanoscale*, 2013, **5**, 8752-8780.
- [24] M. M. Shirolkar, C. Hao, X. Dong, T. Guo, L. Zhang, M. Li and H. Wang, *Nanoscale*, 2014, **6**, 4735-4744.
- [25] Y. Du, Z. X. Cheng, X. L. Wang, P. Liu, S. X. Dou, *J. App. Phys.*, 2011, **109**, 07B507-3.
- [26] J. L. O. Quinonez, D. Diaz, I. Z. Dube, H. A. Santamaria, I. Betancourt, P. S. Jacinto, N. N. Etzana, *Inorganic Chemistry*, 2013, **52** (18), 10306-10316.
- [27] L. A. Fang, J. A. Liu, S. Ju, F. G. Zheng, W. Dong, M. R. Shen, *Appl. Phys. Lett.*, 2010, **97**, 242501-3.
- [28] D. P. Dutta, B. P. Mandal, R. Naik, G. Lawes, A. K. Tyagi, *J. Phys. Chem. C*, 2013, **112**, 2382-2389.
- [29] I. Hernandez-Perez, A. M. Maubert, Luis Rendn, Patricia Santiago, H. Herrera-Hernandez, L. Daz-Barriga Arceo, V. Garibay Febles, Eduardo Palacios Gonzalez, L. Gonzalez-Reyes *Int. J. Electrochem. Sci.*, 2012, **112**, 8832-8847.
- [30] K. R. Gopi and R. Nagarajan, *IEEE Transactions on Nanotechnology*, 2008, **7**(5) 532-7.
- [31] K. A. Kusters, S. E. Pratsinisap, S. G. Thorna, D. M. Smith, *Powder Technology*. 1994, **80**(3), 253-63.
- [32] M. D. Kass, *Materials Letters*, 2000, **42**(4) 246-50.
- [33] Y. Y. Huang, T. P. J. Knowles, and E. M. Terentjev, *Advanced Materials*, 2009 **21**(38-39), 3945-8.
- [34] M. A. Basith, O. Kurni, M. S. Alam, B. L. Sinha, B. Ahmmad, *J. Appl. Phys.*, 2014, **115**, 024102-7.
- [35] I. O. Troyanchuk, A. N. Chobot, O. S. Mantytskaya, N. V. Tereshko, *Inorg. Mater.*, 2010, **46**, 424-428.
- [36] G. S. Lotey, N. K. Verma, *J. Nanopart. Res.* 2012, **14**, 742-748.
- [37] Z. R. Dai, S. Sun, Z. L. Wang, *Surf. Sci.*, 2002, **505**, 325.
- [38] J. Sort, S. Surinach, S. Munoz, M. D. Baro, M. Wojcik, E. Jedryka, S. Nadolski, N. Sheludko, and J. Nogues, *Phys. Rev. B*, 2003, **68**, 014421.
- [39] A. Recnik, I. Nyi-Ksa, I. Ddony, M. Psfai, *CrystEngComm*, 2013, **15**, 7539.
- [40] J. S. Taurozzi, V.A. Hackley, M. R. Wiesner, *Nanotoxicology*, 2011 **5**(4), 71129.
- [41] J. J. Neumeier, H. Terashita, *Phys. Rev. B.*, 2004, **70**, 214435-7.
- [42] D. Lebeugle, D. Colson, A. Forget, M. Viret, P. Bonville, J. F. Marucco, S. Fusil, *Phys. Rev. B.*, 2007, **76**, 024116-8.
- [43] R. Guo, L. Fang, W. Dong, F. Zheng, M. Shen, *J. Phys. Chem. C*, 2010, **114**, 21390-21396.
- [44] K. Singh, R. K. Kotnala, M. Singh, *App. Phys. Lett.* 2008, **93**, 212902-3.
- [45] D. P. Dutta, B. P. Mandal, M. D. Mukadam, S. M. Yusuf, A. K. Tyagi, *Dalton Trans.*, 2014, **43**, 7838-7846.
- [46] S. R. Shannigrahi, A. Huang, N. Chandrasekhar, D. Tripathy, A. O. Adeyeye, *Appl. Phys. Lett.* 2007, **90**, 022901.
- [47] Y. Wang, Y. Li, C. Rong and J. P. Liu, *Nanotechnology*, 2007, **18**, 465701.
- [48] The-Long Phan, *New Physics: Sae Mulli*, 2013, **63**, 557-561.
- [49] S. Roy, I. Dubenko, D. D. Ederh, and N. Ali, *J. Appl. Phys.* 2004 **96** 1202-1208.
- [50] V. M. Chakka, B. Altuncevahir, Z. Q. Jin, Y. Li and J. P. Liu, *J. Appl. Phys.* 2006 **99** 08E912.
- [51] A.R. Makhdoom, M. J. Akhtar, M. A. Rafiq, M. M. Hassan, *Ceramics International*, 2012, **38**, 3829-3834.
- [52] R. Das, T. Sarkar, K. Mandal, *J. Phys. D: Appl. Phys.* 2012, **45**, 455002-12.
- [53] P. Uniyal, K.L. Yadav, *Materials Letters*, 2008 **62**, 2858.
- [54] U. Teipel, K. Leisinger, I. Mikonsaari, *International Journal of Mineral Processing*. 2004 **74** S183-S190.